

# Formation of ultracold LiCs molecules

S D Kraft, P Staunum ‡, J Lange, L Vogel, R Wester and  
M Weidemüller

Physikalisches Institut, Universität Freiburg, Hermann-Herder-Straße 3, 79104  
Freiburg, Germany

E-mail: [stephan.kraft@physik.uni-freiburg.de](mailto:stephan.kraft@physik.uni-freiburg.de)

## Abstract.

We present the first observation of ultracold LiCs molecules. The molecules are formed in a two-species magneto-optical trap and detected by two-photon ionization and time-of-flight mass spectrometry. The production rate coefficient is found to be in the range  $10^{-18} \text{ cm}^3\text{s}^{-1}$  to  $10^{-16} \text{ cm}^3\text{s}^{-1}$ , at least an order of magnitude smaller than for other heteronuclear diatomic molecules directly formed in a magneto-optical trap.

## Introduction

Owing to their permanent electric dipole moment, ultracold heteronuclear dimers offer many exciting possibilities for studies of interacting dipolar gases. At ultralow temperatures the interaction energy of polar molecules in an electric field can largely exceed their thermal energy. Hence processes such as elastic and inelastic collisions can be manipulated by applying electric fields [1, 2, 3, 4]. On the one hand, an array of cold polar molecules has been proposed to represent a quantum computation device, where each qubit is defined by the orientation of a molecular dipole relative to an external electric field [5]. On the other hand, chemical reactions of polar molecules at vanishing thermal energy have been proposed to be controllable by suitable external electromagnetic fields [4, 6]. Despite the existence of potential energy barriers, such reactions feature significant rate coefficients at low temperatures in the Wigner threshold regime [7, 8]. Interesting complementary trapping concepts for polar molecules are electrostatic [12, 13], magnetic [14] and microwave traps [15]. Experimentally, inelastic ultracold homonuclear atom-molecule collisions have been studied in optical dipole traps [9, 10, 11]. Inelastic and elastic collisions involving polar molecules are now open for similar investigations offering new perspectives.

Large molecular electric dipole moments are required in order to make experiments on dipole-dipole interactions and electric field control of ultracold polar molecules feasible. At the current state-of-the-art, heteronuclear alkali dimers seem to be particularly suited. Such ultracold polar dimers can be formed by photoassociation from ultracold samples of their atomic constituents as demonstrated for RbCs [21], KRb [14, 22], and NaCs [23]. The dimer LiCs is predicted to have the largest dipole moment of about 5.5 Debye for low lying vibrational states of the  $X^1\Sigma^+$

‡ Also at: Institut für Quantenoptik, Universität Hannover, Welfengarten 1, 30167 Hannover, Germany

electronic ground state [16, 17]. Recent theoretical studies demonstrate the possibility for manipulating Li-Cs collisions [18], rovibrational dynamics of LiCs molecules [19], binary inelastic collisions between KRb or RbCs [3] and implementing the mentioned quantum computation proposal using optically trapped KRb or RbCs [20].

Here we present the first observation of ultracold LiCs molecules. These are formed out of an ultracold gas of Li and Cs atoms in two spatially overlapped magneto-optical traps (MOTs). As observed in several experiments, homonuclear [24, 25, 26] and heteronuclear [22, 23] alkali dimers can be formed 'directly' in the MOT, i.e., without applying a dedicated photoassociation laser. The molecule formation is generally attributed to photoassociation induced by the trapping laser light [27]; three-body recombination has also been conjectured as a possible cause for ultracold molecule formation in a MOT [24]. In photoassociation by the trapping light, a colliding atom pair is excited at long range to a molecular potential which asymptotically correlates to one excited atom and one ground state atom. Subsequently, the excited molecule decays into two free atoms or into the molecular electronic ground state, thus forming an ultracold dimer in the latter process. According to the semi-classical model by Wang and Stwalley [28] the probability for the excitation step is proportional to the reduced mass of the molecule to the power of 9/4, which yields a significant reduction for LiCs as compared, e.g., to NaCs for which molecule formation rates around  $10 - 100 \text{ s}^{-1}$  were observed in a MOT. In fact, light-induced inelastic collisions between ground state Li and excited state Cs atoms in a two-species MOT have been observed by our group as a source of substantial atom loss already some years ago [29]. The loss is due to the large kinetic energy gained by moving inwards on the excited state potential curve [30] and possibly partly due to formation of LiCs molecules. In this work, using a dedicated scheme for the detection of LiCs molecules in the electronic ground state, we show that ground state LiCs molecules are indeed formed in a two-species MOT and we estimate their production rate.

### Two-species magneto-optical trap

The LiCs molecules are formed from Li and Cs atoms trapped in two overlapped magneto-optical traps. The laser light for the Li MOT is provided by two injection locked diode lasers (Philips, CQL-806), one detuned 20 MHz below the  $F=2$  to  $F'=3$  transition of the D2 line for cooling, the other tuned to the  $F=1$  to  $F'=2$  transition for repumping. The two beams are combined on a beamsplitter. Three mutually perpendicular and retroreflected beams (4 mW power in each horizontal beam and twice the power in the vertical direction; 18 mm diameter), derived from the combined beam, form the MOT. The Cs MOT is formed by one retroreflected beam in the vertical direction and four pairwise counterpropagating beams in the horizontal plane. Each horizontal beam has a power of 4 mW (twice as much for the vertical beam) and a diameter of 16 mm. The cooling light is provided by a DBR laser diode (SDL-5722-H1), which is locked 16 MHz to the red of the  $F=4$  to  $F'=5$  transition near 852 nm. A second diode laser (SDL-5712-H1) is used for repumping from the  $F=3$  state. For optimizing the spatial overlap of the MOTs, the Li and Cs MOT laser beams are adjusted separately while observing the fluorescence light of both MOTs in two perpendicular planes using two CCD cameras. The central part of the experiment is sketched in Fig. 1.

Both MOTs are loaded from Zeeman slowed atomic beams coming out of a two-

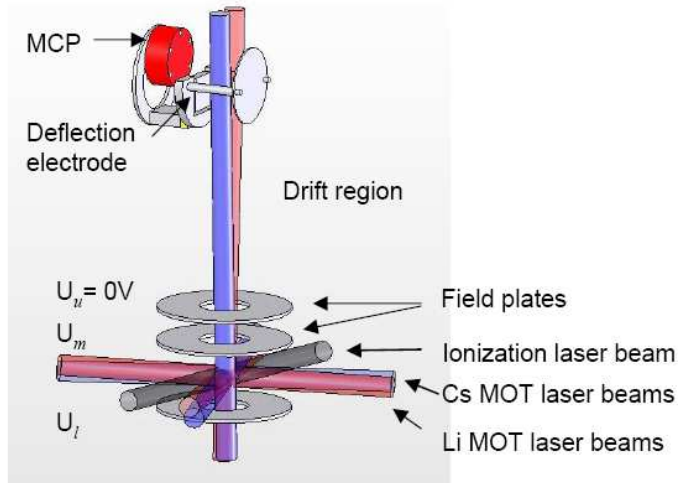


**Figure 1.** Sketch (not to scale) of the central part of the two-species magneto-optical trap with time-of-flight mass spectrometer of Wiley-McLaren type. Ions produced by photoionization of trapped atoms and molecules between the two lower field plates are accelerated upwards. After 30 cm they are deflected off the vertical axis onto a microchannel plate detector (MCP).

species oven, which consists of two separate chambers connected by a capillary [31]. Each chamber can be heated separately and hence the flux of the two atomic species can be controlled independently. The front chamber containing Li is heated to 350°C while the rear chamber containing Cs has a temperature of 150°C. The oven nozzle and the capillary are kept at 365°C to prevent clogging. The Li (Cs) Zeeman slower laser is detuned 76 MHz (24 MHz) below the cooling transition. Under these conditions we achieve loading rates of  $5 \times 10^7 \text{ s}^{-1}$  and  $1 \times 10^8 \text{ s}^{-1}$  for the Li and the Cs MOT, respectively. Under steady-state conditions,  $1.5 \times 10^8$  Li atoms and  $1.5 \times 10^8$  Cs atoms are trapped at a density of  $1 \times 10^{10} \text{ cm}^{-3}$  and  $5 \times 10^9 \text{ cm}^{-3}$ , respectively. Due to light-induced inelastic collisions [29], the number of trapped atoms is reduced to 75 % for Lithium as well as Cesium as compared to trapping only a single species in the MOT.

### Time-of-flight mass spectrometer

To sensitively detect small numbers of molecules in an atomic gas, pulsed two-photon ionization is combined with time-of-flight mass spectrometry. The laser pulses are delivered by a pulsed dye laser (Radiant Dyes Narrowscan with 7 ns pulse width and 13 mJ energy per pulse). Based on ab initio potentials [32] and previous spectroscopic studies in a heat pipe [33] an ionization wavelength range near 680 nm was chosen to achieve resonantly enhanced two-photon ionization of LiCs. The pulsed dye laser beam is expanded to a  $1.5 \text{ cm}^2$  cross sectional area in order to have a large ionization volume. The laser pulses produce a significant atomic ion yield on the detector by non-resonantly ionizing both Li and Cs atoms from the magneto-optical traps, either with two photons from the  $2p_{3/2}$  and  $6p_{3/2}$  states, respectively, or with three photons from the atomic ground states. To separate a small signal of  $\text{LiCs}^+$  from a large signal of  $\text{Cs}^+$ , a high mass resolution is required. For this purpose we implemented a

Wiley-McLaren time-of-flight mass spectrometer (see Fig. 1 and Refs. [34, 35]).

Upon formation, all ions are accelerated upwards by applying voltages to the field plates as indicated in Fig. 1. After passing a 30 cm drift region they are deflected onto a microchannel plate detector (MCP) placed off the vertical axis in order to allow optical access along this axis. By suitably adjusting the ratio between the voltages on the lower ( $U_l$ ) and the middle ( $U_m$ ) field plate as well as the voltage on the deflection electrode ( $U_{defl}$ ), the ions are time-focused onto the detector, i.e., ions of the same mass arrive at the MCP within a narrow time interval even though they are formed at different positions within the ionization volume. The resulting voltage pulse from the MCP, due to  $\text{Cs}^+$  ions formed by ionization of atoms from the MOT, appears at a time  $\tau_{\text{Cs}} = 12.74 \mu\text{s}$  after the laser pulse and is about 50 ns wide. The  $\text{Cs}_2^+$  ion peak is slightly broader (70 ns), since the molecular ions are produced in a much larger volume than the ions originating from trapped Cs atoms. The mass difference between  $\text{LiCs}^+$  and  $\text{Cs}^+$  of 5% leads to a difference in time of flight (scaling as  $\sqrt{\text{mass}}$ ) of only 2.5%. We therefore expect the  $\text{LiCs}^+$  peak to appear at  $\tau_{\text{LiCs}} = 13.07 \mu\text{s}$ , roughly 300 ns after the  $\text{Cs}^+$  peak, with a similar width as the  $\text{Cs}_2^+$  peak.

Since the Cs MOT contains many more atoms than LiCs molecules are expected to be formed, it is necessary to suppress the  $\text{Cs}^+$  signal as much as possible. In order to avoid two-photon ionization of  $\text{Cs}(6p_{3/2})$  atoms we block the laser beams of the Cs MOT and of the Cs Zeeman slower in a 2 ms period before the dye laser pulse arrives, using mechanical shutters. During this period all excited Cs atoms decay to the electronic ground state and hence only three-photon ionization of  $\text{Cs}(6s_{1/2})$  is possible. With this scheme we suppress the  $\text{Cs}^+$  signal by a factor of 50, resulting in about one detected  $\text{Cs}^+$  ion per dye laser pulse.

### Detection of LiCs molecules

In a first set of measurements we record time-of-flight traces with the dye laser wavelength set to 682.78 nm. Fig. 2(a) shows an oscilloscope image recorded with only the Cs MOT present, the laser beams of Li MOT and Li Zeeman slower being blocked. In the upper part of the image the MCP voltage of about 1100 time-of-flight traces laid on top of each other is shown. The lower curve is an average over all traces. Every time an ion hits the MCP detector a dip in the voltage is observed. On both images we observe a large 50 ns wide peak centered at  $12.74 \mu\text{s}$  originating from about one  $\text{Cs}^+$  ion per dye laser pulse, produced by non-resonant three-photon ionization of Cs MOT atoms.

Additionally, we find a broad background of ions around the  $\text{Cs}^+$  peak in a time interval from 300 ns before to 200 ns after the  $\text{Cs}^+$  arrival time. The detection rate of such background ions is about one per ten dye pulses and therefore constitutes an important source of background events near the expected  $\text{LiCs}^+$  peak. These ions can be attributed to fast  $\text{Cs}^+$  ions formed by ionization of fast Cs atoms: Weakly bound electronic ground state  $\text{Cs}_2$  molecules (formed by photoassociation induced by Cs MOT light) are photodissociated by a first dye laser photon. After dissociation the two atoms are either in the  $\text{Cs}(6s_{1/2})$  and  $\text{Cs}(6p_{3/2})$  or in the  $\text{Cs}(6s_{1/2})$  and  $\text{Cs}(6p_{1/2})$  states. Depending on the state they each have a kinetic energy of 0.18 eV or 0.22 eV, respectively. The resulting  $\text{Cs}(6p)$  atom is then ionized by two-photon ionization.  $\text{Cs}^+$  ions emerging from this process have a velocity of about 500 m/s and 550 m/s, respectively, which leads to a broad distribution as observed in the measured time-of-flight trace. To avoid the fast  $\text{Cs}^+$  ion background at the expected arrival time of the

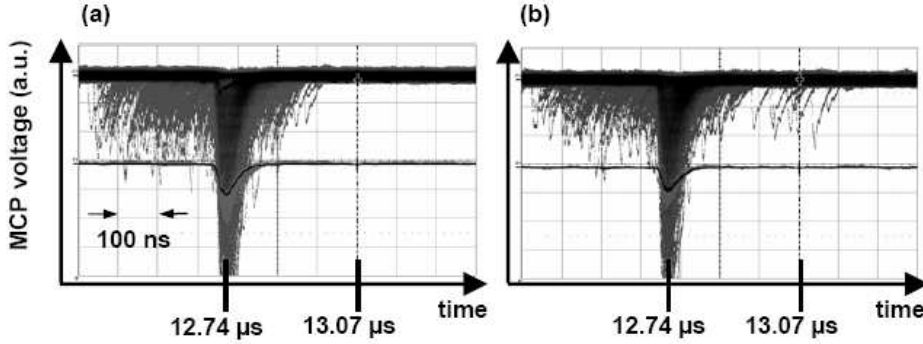


**Figure 2.** Oscilloscope images of time-of-flight traces for photoionisation (a) in a single-species Cs MOT, and (b) in a two-species Li-Cs MOT. The upper part of each image shows about 1100 time-of-flight traces on top of each other. The lower curve represents an average of the traces. The  $\text{Cs}^+$  ions arrive at  $12.74 \mu\text{s}$ , the  $\text{LiCs}^+$  ions around  $13.07 \mu\text{s}$ .

$\text{LiCs}^+$  ions, we reduced its width to  $\Delta\tau = 500 \text{ ns}$  by applying large absolute voltages  $U_l$  and  $U_m$  to the field plates, which in turn decreases the ratio  $\frac{\Delta\tau}{\tau_{\text{LiCs}^+} - \tau_{\text{Cs}^+}}$ .

In addition, the arrival time of the fast ions can be shifted to shorter arrival times relative to the narrow  $\text{Cs}^+$  peak by adjusting the ratio of the field plate voltages ( $U_l/U_m$ ) at the cost of a slightly non-optimal time-focussing. By applying these fine-adjustments to the field plates, we can clearly separate the fast  $\text{Cs}^+$  ion background from ions at the expected  $\text{LiCs}^+$  arrival time. More specifically, at  $U_l=800 \text{ V}$ ,  $U_m=610 \text{ V}$  and  $U_{\text{defl}}=1990 \text{ V}$  the rate of  $\text{Cs}^+$  ions appearing within 100 ns of the expected  $\text{LiCs}^+$  arrival time at  $13.07 \mu\text{s}$  is about one ion per 4500 dye pulses.

In Fig. 2(b), recorded with both MOTs being present, we observe several ions in excess of the  $\text{Cs}^+$  background, which impact on the detector at the expected  $\text{LiCs}^+$  arrival time, in addition to the  $\text{Cs}^+$  peak and a broad background as in Fig. 2(a). These ions are only observed when both the Li and the Cs MOTs are present. In a window of 100 ns width around the expected  $\text{LiCs}^+$  arrival time four ion signals are counted in 1100 dye pulses. To exclude that these ions are produced by processes induced by the Li trapping light at 670 nm, such as photodissociation of  $\text{Cs}_2$ , we compared the measurements in Fig. 2(a), where all Li lasers are blocked, to measurements with the Li MOT laser beams present but the Li Zeeman slower laser beam being blocked, i.e. with no Li atoms being loaded into the MOT. In both cases only about one ion every 4500 cycles appears within a 100 ns window at the expected  $\text{LiCs}^+$  arrival time. Thus, we conclude that the ions observed in Fig. 2(b) at a much larger rate originate from cold LiCs molecules formed out of cold Li and Cs atoms in the two-species MOT.

Photoassociation of LiCs molecules induced by the laser light can only occur via the  $\text{Li}(2s_{1/2})+\text{Cs}(6p_{3/2})$  asymptote. Photoassociation to potentials correlating to the  $\text{Li}(2p_{3/2})+\text{Cs}(6s_{1/2})$  asymptote is excluded since all potentials are repulsive beyond  $50 \text{ \AA}$ , with the exception of one potential curve which is slightly attractive and supports a potential minimum around  $70 \text{ \AA}$ . However, this potential well is extremely shallow so that photoassociation into this well is not possible since the Li laser detunings are much larger than the well depth [36]. Since the Cs MOT and Zeeman slower laser light is blocked in a 2 ms period before the ionization pulse, all molecules formed via

the  $\text{Li}(2s_{1/2})+\text{Cs}(6p_{3/2})$  asymptote must have decayed to the electronic ground state before ionization. In the case of LiCs formation by three-body recombination, which is unlikely due to the comparatively small pair densities, the molecules would be formed directly in the electronic ground state. In either case, the detected  $\text{LiCs}^+$  ions arise from ultracold LiCs molecules in the electronic ground state.

The 2 ms time interval between the blocking of the Cs MOT lasers and the ionization pulse gives an upper bound on the velocity of the molecules. Only molecules can be ionized which have not left the ionization region resulting in a maximal velocity of 5 m/s. However, the corresponding temperature of 0.3 K can only be seen as an upper bound. Based on other experiments with KRb and NaCs [22, 23] we expect a temperature for LiCs on the order of  $100 \mu\text{K}$  given by the Cs temperature.

Within the measured 1100 dye laser pulses, we detect  $(3.6 \pm 2.0) \times 10^{-3}$  LiCs ground state molecules per ionization pulse after background subtraction and assuming Poissonian statistical uncertainties. In order to estimate the LiCs production rate several factors must be taken into account. Due to gravity and finite kinetic energy the molecules leave the ionization volume. Therefore, they can be ionized only in an interval of 13 ms after their production. Due to the 10 Hz repetition rate of the ion detection, only 13% of the produced molecules are available for ionization. Additionally, our detector is estimated to have a detection efficiency of about 20% [34]. Assuming that all molecules within the laser field of the dye pulse are ionized, we derive a production rate of  $0.14 \pm 0.08$  molecular ions per second. As the ionization process has not yet been investigated, the ionization probability is estimated to lie between 10% and 0.1%, depending on the proximity of the dye laser wavelength to an intermediate resonance state. This leads us to an estimate of the actual molecule production rate between  $1.4 \pm 0.8$  and  $140 \pm 80$  LiCs molecules per second.

In our experiments the Li MOT is larger than the Cs MOT. In this case the molecular production rate can be approximately written as

$$dN_{\text{LiCs}}/dt = \beta_{\text{LiCs}} N_{\text{Cs}} n_{\text{Li}}$$

where  $N_{\text{Cs}}$  is the total number of Cs atoms,  $n_{\text{Li}}$  the Li peak density and  $\beta_{\text{LiCs}}$  the rate coefficient of LiCs molecule production. With typical values of our double MOT setup of  $n_{\text{Li}} = 10^{10} \text{ cm}^{-3}$  and  $N_{\text{Cs}} = 1.5 \times 10^8$  this leads to a molecule production rate coefficient between  $10^{-18} \text{ cm}^3\text{s}^{-1}$  and  $10^{-16} \text{ cm}^3\text{s}^{-1}$  for 10% and 0.1% ionization probability, respectively. A similar range of production rate coefficients results from a second set of measurements, which we performed with a smaller Li MOT at a dye laser wavelength of 681.08 nm. The obtained range of rate coefficients is in agreement with the calculated Franck-Condon factors for polar alkali dimer photoassociation [28]. This calculation predicts for LiCs a rate coefficient of about an order of magnitude smaller as compared to the formation rate of NaCs measured as  $10^{-15} \text{ cm}^3\text{s}^{-1}$  in a MOT [23]. Both the LiCs and the NaCs formation rates are much smaller than the observed rate for photoassociation of KRb in the trapping light, measured to be  $8 \times 10^{-12} \text{ cm}^3\text{s}^{-1}$  [22], due to the much larger Franck-Condon factor in the KRb system.

## Conclusion

We report on the first detection of ultracold LiCs molecules in the electronic ground state. The molecule formation rate coefficient is estimated to be between  $10^{-18} \text{ cm}^3\text{s}^{-1}$  and  $10^{-16} \text{ cm}^3\text{s}^{-1}$ . This coefficient is smaller than the values obtained for NaCs and KRb [22, 23], which can be essentially explained by the small reduced mass of LiCs

and the very large  $C_6$  coefficients for KRb [28, 36]. Future experiments on LiCs will therefore include photoassociation with a tunable cw Ti:Sapphire laser either in the two-species MOT or an optical dipole trap [37], which should lead to LiCs production rates larger by orders of magnitude [38]. Furthermore, ionization spectra as a function of the dye laser wavelength will be measured to analyze the vibrational state distribution of the formed molecules. By transferring the formed molecules to low lying vibrational states of the  $X^1\Sigma^+$  state by stimulated Raman processes [39] or using microwave fields, cold polar molecules with electric dipole moment as large as 5.5 Debye [17] can be obtained for studies on dipolar gases and ultracold chemistry.

This work was supported by the Deutsche Forschungsgemeinschaft in the frame of the Schwerpunktprogramm 1116 and by the European Commission in the frame of the Cold Molecule Research Training Network under contract HPRN-CT-2002-00290.

## References

- [1] J. Bohn. Inelastic collisions of ultracold polar molecules. *Phys. Rev. A*, 63:052714, 2001.
- [2] C. Ticknor and J. Bohn. Long-range scattering resonances in strong-field-seeking states of polar molecules. *Phys. Rev. A*, 72:032717, 2005.
- [3] A. Avdeenkov, M. Kajita, and J. Bohn. Suppression of inelastic collisions of polar  $^1\Sigma$  state molecules in an electrostatic field. *Phys. Rev. A*, 73:022707, 2006.
- [4] R. Krems. Molecules near absolute zero and external field control of atomic and molecular dynamics. *Int. Rev. Phys. Chem.*, 24:99–118, 2005.
- [5] D. DeMille. Quantum computation with trapped polar molecules. *Phys. Rev. Lett.*, 88:067901, 2002.
- [6] A. Avdeenkov and J. Bohn. Linking ultracold polar molecules. *Phys. Rev. Lett.*, 90:043006, 2003.
- [7] N. Balakrishnan and A. Dalgarno. Chemistry at ultracold temperatures. *Chem. Phys. Lett.*, 341:652–656, 2001.
- [8] E. Bodo, F. Gianturco, and A. Dalgarno. F+D<sub>2</sub> reaction at ultracold temperatures. *J. Chem. Phys.*, 116:9222–9227, 2002.
- [9] P. Staantum, S. D. Kraft, J. Lange, R. Wester, and M. Weidemüller. Experimental investigation of ultracold atom-molecule collisions. *Phys. Rev. Lett.*, 96:023201, 2006.
- [10] N. Zahzam, T. Vogt, M. Mudrich, D. Comparat, and P. Pillet. Atom-molecule collisions in an optically trapped gas. *Phys. Rev. Lett.*, 96:023202, 2006.
- [11] G. Thalhammer, K. Winkler, F. Lang, S. Schmid, R. Grimm, and J. Hecker Denschlag. Long-lived Feshbach molecules in a three-dimensional optical lattice. *Phys. Rev. Lett.*, 96:050402, 2006.
- [12] S. Y. T. van de Meerakker, P. H. M. Smeets, N. Vanhaecke, R. T. Jongma, and G. Meijer. Deceleration and electrostatic trapping of OH radicals. *Phys. Rev. Lett.*, 94:023004, 2005.
- [13] T. Rieger, T. Junglen, S. Rangwala, P. Pinkse, and G. Rempe. Continuous loading of an electrostatic trap for polar molecules. *Phys. Rev. Lett.*, 95:173002, 2005.
- [14] D. Wang, J. Qi, M. F. Stone, O. Nikolayeva, H. Wang, B. Hattaway, S. D. Gensemer, P. L. Gould, E. E. Eyler, and W. C. Stwalley. Photoassociative production and trapping of ultracold KRb molecules. *Phys. Rev. Lett.*, 93:243005, 2004.
- [15] D. DeMille, D. Glenn, and J. Petricka. Microwave traps for cold polar molecules. *Eur. Phys. J. D*, 31:375–384, 2004.
- [16] G. Igel-Mann, U. Wedig, P. Fuentealba, and H. Stoll. Ground-state properties of alkali dimers xy (x,y=Li to Cs). *J. Chem. Phys.*, 84:5007–5012, 1986.
- [17] M. Aymar and O. Dulieu. Calculation of accurate permanent dipole moments of the lowest  $^1,3\Sigma^+$  states of heteronuclear alkali dimers using extended basis sets. *J. Chem. Phys.*, 122:204302, 2005.
- [18] R. Krems. Controlling collisions of ultracold atoms with dc electric fields. *Phys. Rev. Lett.*, 96:123202, 2006.
- [19] R. Gonzalez-Ferez, M. Mayle, and P. Smelcher. Rovibrational dynamics of LiCs dimers in strong electric fields. Submitted for publication.
- [20] S. Kotochigova and E. Tiesinga. Controlling polar molecules in optical lattices. *Phys. Rev. A*, 73:041405(R), 2006.

- [21] A. Kerman, J. M. Sage, S. Sainis, T. Bergeman, and D. DeMille. Production and state-selective detection of ultracold RbCs molecules. *Phys. Rev. Lett.*, 92:153001, 2004.
- [22] M. W. Mancini, G. D. Telles, A. R. L. Caires, V. S. Bagnato, and L. G. Marcassa. Observation of ultracold ground-state heteronuclear molecules. *Phys. Rev. Lett.*, 92:133203, 2004.
- [23] C. Haimberger, J. Kleinert, M. Bhattacharya, and N. P. Bigelow. Formation and detection of ultracold ground-state polar molecules. *Phys. Rev. A*, 70:021402(R), 2004.
- [24] C. Gabbanini, A. Fioretti, A. Lucchesini, S. Gozzini, and M. Mazzoni. Cold rubidium molecules formed in a magneto-optical trap. *Phys. Rev. Lett.*, 84:2814–2817, 2000.
- [25] A. Fioretti, D. Comparat, A. Crubellier, O. Dulieu, F. Masnou-Seeuws, and P. Pillet. Formation of cold Cs<sub>2</sub> molecules through photoassociation. *Phys. Rev. Lett.*, 80:4402–4405, 1998.
- [26] T. Takekoshi, B. M. Patterson, and R. J. Knize. Observation of optically trapped cold cesium molecules. *Phys. Rev. Lett.*, 81:5105–5108, 1998.
- [27] A. Caires, V. Nascimento, D. Rezende, V. Bagnato, and L. Marcassa. Atomic density and light intensity dependences of the Rb<sub>2</sub> molecule formation rate constant in a magneto optical trap. *Phys. Rev. A*, 71:043403, 2005.
- [28] H. Wang and W. C. Stwalley. Ultracold photoassociative spectroscopy of heteronuclear alkali metal dimers. *J. Chem. Phys.*, 108:5767, 1998.
- [29] U. Schlöder, H. Engler, U. Schünemann, R. Grimm, and M. Weidemüller. Cold inelastic collisions between lithium and cesium in a two-species magneto-optical trap. *Eur. Phys. J. D.*, 73:802, 1999.
- [30] S. Gensemer and P. Gould. Ultracold collisions observed in real time. *Phys. Rev. Lett.*, 80:936–939, 1998.
- [31] C. A. Stan and W. Ketterle. Multiple species atom source for laser-cooling experiments. *Rev. Sci. Instr.*, 76:063113, 2005.
- [32] M. Korek, A. R. Allouche, K. Fakhreddine, and A. Chaalan. Theoretical study of the electronic structure of LiCs, NaCs and KCs molecules. *Can. J. Phys.*, 78:977–988, 2000.
- [33] A. Pashov, P. Sta anum, H. Knöckel, and E. Tiemann. In preparation.
- [34] S. D. Kraft, J. Mikosch, P. Sta anum, A. Fioretti, J. Lange, R. Wester, and M. Weidemüller. A time-of-flight mass spectrometer for experiments with ultracold gases. arXiv:physics/0504079.
- [35] W. C. Wiley and I. H. McLaren. Time-of-flight mass spectrometer with improved resolution. *Rev. Sci. Instr.*, 26:1150–1157, 1955.
- [36] B. Bussery, Y. Achkar, and M. Aubert-Frécon. Long-range molecular states dissociating to the three or four lowest asymptotes for the ten heteronuclear diatomic alkali molecules. *Chem. Phys.*, 116:319–338, 1987.
- [37] M. Mudrich, S. Kraft, K. Singer, R. Grimm, A. Mosk, and M. Weidemüller. Sympathetic cooling with two atomic species in an optical trap. *Phys. Rev. Lett.*, 88:253001, 2002.
- [38] S. Azizi, M. Aymar, and O. Dulieu. Prospects for the formation of ultracold ground state polar molecules from mixed alkali atom pairs. *Eur. Phys. J. D*, 31:195–203, 2004.
- [39] J. M. Sage, S. Sainis, T. Bergeman, and D. DeMille. Optical production of ultracold polar molecules. *Phys. Rev. Lett.*, 94:203001, 2005.